Performance of geobarrier system under rainfall infiltration

Harianto Rahardjo, Nurly Gofar & Alfrendo Satyanaga
School of Civil and Environmental Engineering, Nanyang Technological University, Singapore

ABSTRACT: A Geobarrier system (GBS) is a retaining structure comprising geobags and utilizing capillary barrier principles to act as a protection of steep slope against rainfall-induce slope failures. Capillary barrier principles harness the distinct difference in unsaturated hydraulic properties between a fine-grained layer and a coarse-grained layer. In this study, the performance of GBS as a protection of a steep residual soil slope was investigated. The GBS was constructed using recycled materials and it was planted with vegetation to provide green cover and to blend in with the surrounding environment. Finite element analyses were carried out to evaluate the earth pressure and pore-water pressure variations within and behind the GBS slope during and after rainfall. Limit equilibrium analyses were performed at various stages during and after rainfall to assess the near vertical wall stability. The results of the deformation and seepage analyses showed that the reinforced zone in the GBS remained unsaturated during rainfall, indicating that the GBS slope performed well in minimizing the rainwater infiltration.

Keywords: GeoBarrier System, rainfall infiltration, pore-water pressure, deformation, recycled material, geobag, geogrids

1 INTRODUCTION

Rapid infrastructure development in Singapore have resulted in demand for excavation of original slopes to a steeper angle. These engineered slopes need to adopt suitable measures to prevent failures by recognizing the possible factors leading to instability. One possible cause of slope instability in tropical areas is rainfall infiltration. Reinforced soil walls have been used to stabilize the near vertical slopes because it requires less cutting and filling, reduces construction time and it is usually more cost effective. This method offers mechanical stabilization of the near vertical slopes, but the performance of this type of wall depends primarily on the quality of fill material, drainage system and construction procedures (Koerner, 2012). Failures of reinforced soil wall triggered by rainfall infiltration have been reported (Yoo and Jung, 2006; Liu et al, 2012; Koerner and Koerner, 2013). Capillary barrier is an effective method to minimize rain water infiltration into soil slopes (Rahardjo et al., 2012). It is a man-made two-layer cover system comprising a fine-grained (moisture retention) layer and a coarse-grained (capillary break) layer of soils (Harnas et al., 2014).

Geobarrier system (GBS) was developed to combine the mechanical stabilization offered by the reinforced soil wall and the protection from rainfall infiltration offered by the capillary barrier system (Rahardjo et al., 2015). For the near vertical slope, the fine material is encapsulated with geobag and connected to geogrids reinforcement, to augment the stability of the slope. The coarse material is laid in between the reinforced soil fill and the geobags of fine materials. Rahardjo et al (2018) showed that the presence of geobags between the fine and coarse material does not interfere the effectiveness of the capillary barrier system.

Previous studies by Rahardjo et al. (2013) and McCulloch et al. (2017) showed that recycled materials can be used to replace natural materials forming the capillary barrier system. Therefore, in line with current sustainable environment policies, recycled materials were used as components of capillary barrier

system in the GBS. Approved soil mixture (ASM) was contained in another geobag and placed on top of the fine-grained layer to facilitate the planting of deep and widespread rooted shrubs/trees. The system was also enhanced with proper drainage system below the toe of the slope.

The performance of the GBS was evaluated under Singapore's tropical climatic conditions through a pilot field study. This paper presents the field data gained from one-year monitoring of the pilot study conducted at the southern part of Singapore in terms of pore-water pressure (PWP) profile and earth pressure variation. Deformation and seepage analyses were carried out to model the response of the GBS to actual rainfall pattern, thus the performance of the GBS slope could be predicted using the numerical model for different conditions related to soil properties and flux boundary conditions.

2 PILOT STUDY

Three GBS slopes were constructed on a residual soil slope in Singapore with different combinations of recycled materials as components of capillary barrier system (Figure 1). The GBS slopes were 4 m high, sloping at 70^{o} to the horizontal, and consisted of eight layers of geobags with a 2.8 m long geogrids reinforcement. Compacted in-situ soil was used as a reinforced soil fill. A 0.3-m thick of coarse material was laid on the reinforced soil fill before the placement of bags of fine RAP. Stacked of geobags of fine material and geobags of ASM served as facing panel of the reinforced slope. Geogrids reinforcements were secured in between two layers of geobags.

The pilot study area was instrumented with a rain-gauge and two Cassagrande-type piezometers to monitor rainfall and groundwater table, respectively. The GBS slopes were instrumented with four pairs of tensiometer and soil moisture sensor for the measurement of negative PWP and volumetric water content (VWC), respectively, during rainwater infiltration. All tensiometers and soil moisture sensors were located at 2 m depth from the crest of the slope and each of them measured the response of different materials (reinforced soil, coarse material and fine material). This paper presents the response of the middle slope (GBS slope 2) because in addition to tensiometers and soil moisture sensors, only this slope was also instrumented with earth pressure cells. The earth pressure cells were installed at a depth of 1.5 m from the crest of the slope to monitor the transient vertical and lateral stresses in response to rainwater infiltration. GBS slope 2 used reclaimed asphalt pavement (RAP) as fine and coarse materials forming the capillary barrier. All instruments (tensiometers, soil moisture sensors, earth-pressure cells, piezometers, rain-gauge) were connected to a data acquisition system (DAS) and sent to a website for remote real-time monitoring. The schematic diagram of GBS slopes and locations of the instruments are shown in Figure 2.

Figure 1 Pilot study of GeoBarrier System (GBS) slope in Singapore

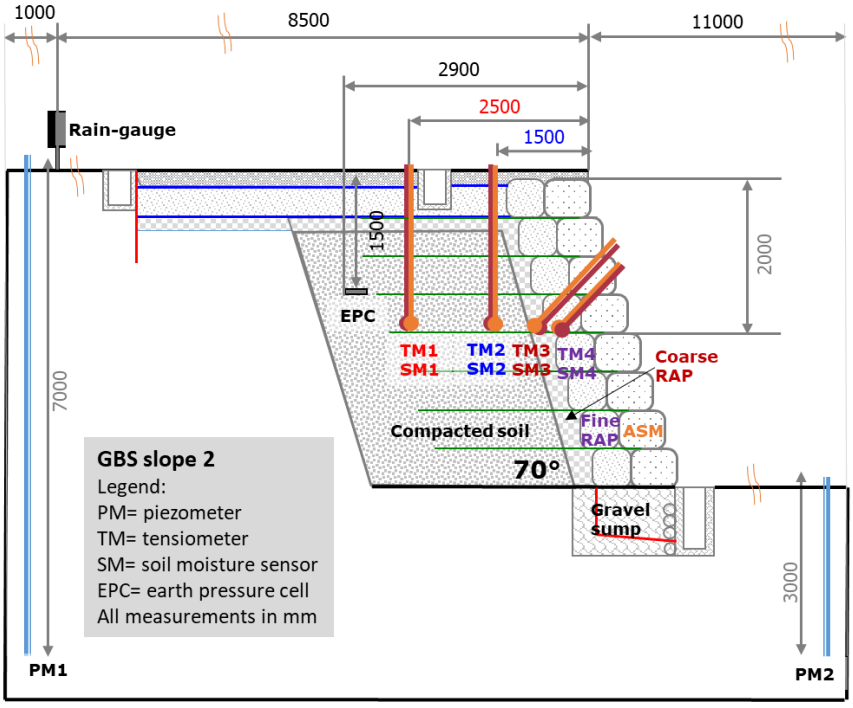

Figure 2. Schematic diagram of GBS slope 2 with instrumentations.

The monitoring period was 1 year from 1st July 2016 to 30th June 2017. The rainfall record for the month of January 2017 (Figure 3) was used in the numerical analyses because the record started with a long dry period, followed by one week of a very wet condition. The rainfall started at 14:20 on 18th January 2017 and the intermittent rainfalls lasted until 23rd January 2017. The cumulative rainfall during this one week period was 204 mm while the highest daily rainfall was 103.8 mm on January 23rd 2017. The maximum hourly rainfall was 38.7mm/h at 10:00am on 23rd January 2017. The plot of hourly rainfall from 00:00 on 18th January 2017 to 23:30 on 23rd January 2017 is shown in the insert of Figure 3. This rainfall was used as the flux boundary condition in the numerical analyses. The initial pore-water pressures within the GBS slope were set as spatial function based on the pore-water pressure measurements (TM1, TM2, TM3, TM4 as indicated in Figure 2) at 00:00 on 18th January2017.

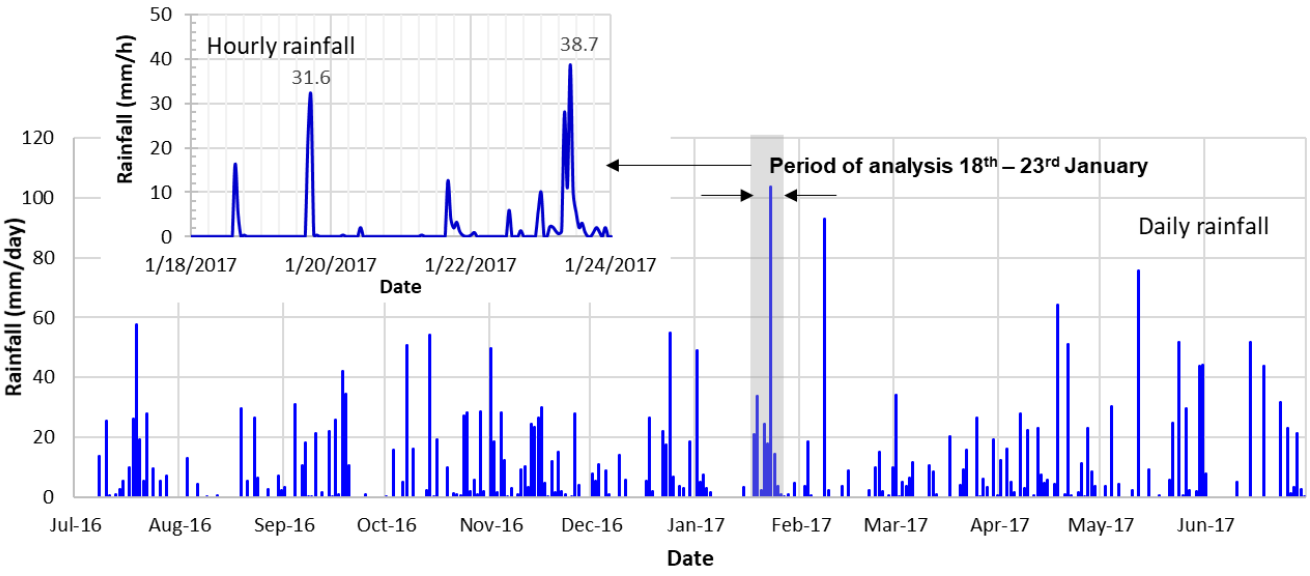

Figure 3. Rainfall records from 1 year monitoring period (1st July 2016 – 30th June 2017) and the rainfall condition analyzed in this study (00:00 on 18th January to 23:50 on 23rd January 2017)

3 DEFORMATION SEEPAGE ANALYSIS

A deformation and seepage analysis was carried out to study the response of GBS slope 2 using SIGMA/W (Geoslope International, 2012). The near vertical slope was subjected to the heavy rainfall condition shown in Figure 3b. The boundary conditions applied to the finite element model are illustrated in Figure 4. The mesh consisted of 3593 rectangular and triangular elements. The left and right boundaries were set at 10 m and 10.7 m from the crest and toe of the slope, respectively, while the bottom boundary was set at 8 m from the ground surface at the toe of the slope. For the deformation analysis, zero vertical displacements were assigned at both vertical boundaries and the bottom of the model. For the seepage analysis, no flow boundaries were simulated by assigning a nodal flux Q equal to zero at the bottom and the sides of the slope model above the ground water level (GWL). A constant total head h_w was applied on each side boundary below GWL. The rainfall was applied to the ground surface as a flux boundary q. Ponding was not allowed to occur on the ground surface, which meant that the PWP was not allowed to be greater than 0 kPa on the ground surface. This condition simulated the actual condition whereby the excess rainwater on the slope would become runoff. Soil-water characteristic curves (SWCC) and permeability functions used for the seepage analysis are shown in Figure 5 while the SWCC fitting parameters and the properties of materials used in the numerical analyses are summarized in Table 1 and Table 2, respectively. The construction sequence adopted in the numerical analyses started with an in-situ condition and placement of eight lifts of reinforced layers and geobags, followed by the application of rainfall on the crest. The results of the numerical analyses were evaluated at time 0 (before rainfall application) and during rainfall (1 day, 2 days, 4 days and 6 days). Global and local stabilities of the slope at these respective stages were evaluated using the limit equilibrium method of Morgenstern and Price in SLOPE/W (Geoslope International, 2012).

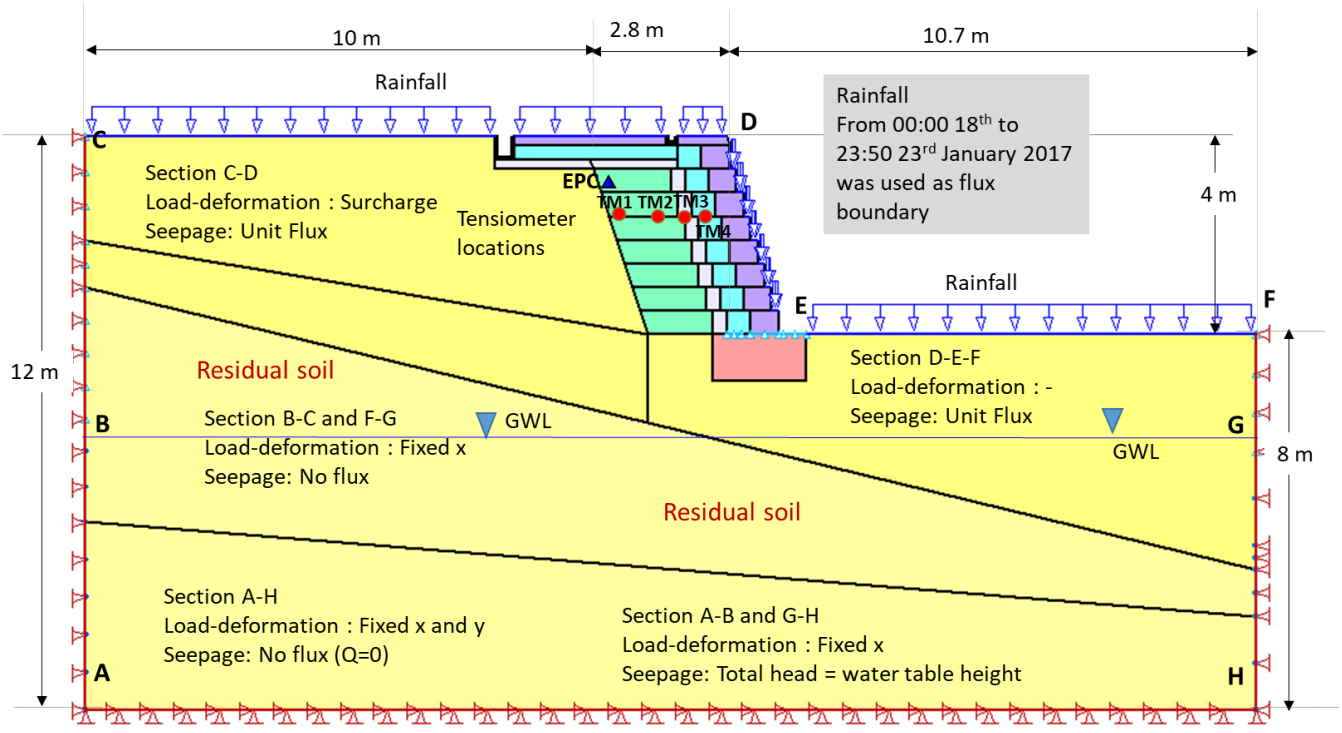

Figure 4 GBS slope for numerical analysis using deformation-seepage analysis in SIGMA/W and slope stability analysis in SLOPE/W

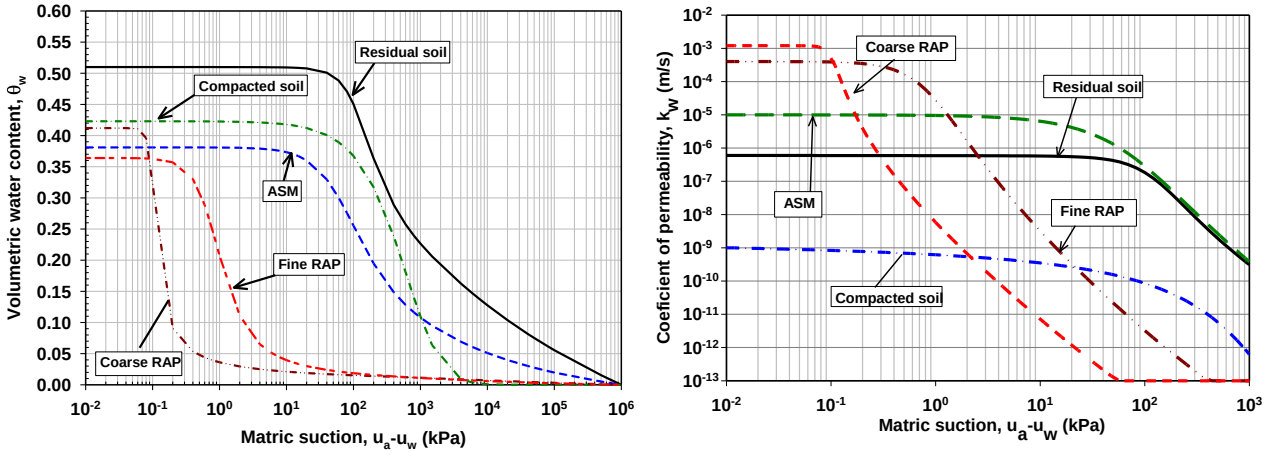

(a) (b)

Figure 5 (a) SWCCs and (b) permeability functions of materials used in seepage analysis.

Table 1 SWCC fitting parameters of materials used in this study

Fitting Parameters of SWCC	ASM	Residual soil	Fine RAP	Coarse RAP	Gravel	Compacted soil
a	56.11	98.5	0.717	0.098	0.11	1630
n	1.55	2.6	2.439	9.619	2.72	1.06
m	0.785	0.41	1.192	0.784	0.79	7

Table 2 Hydraulic and shear strength properties of materials used in this study

Description	Symbol (Unit)	ASM	Residual soil	Fine RAP	Coarse RAP	Gravel	Compacted soil
Effective cohesion	c' (kPa)	2	5	0	0	0	5
Effective friction angle	ϕ' (°)	30	28	34	35	35	38
Air-entry value	ψ_a (kPa)	26	64	0.40	0.09	0.07	112.5
ϕ^b for $0<(u_a-u_w)\leq \psi_a$	ϕ^b (°)	30	28	34	35	35	38
ϕ^b for $(u_a-u_w) > \psi_a$	ϕ^b (°)	15	14	17	17	17	14
Total unit weight	γ (kN/m^3)	16.5	18.0	20.0	21.0	21.0	20.0
Saturated vol. water content	θ_s	0.381	0.51	0.364	0.412	0.39	0.423
Coef. of saturated permeability	ks (m/s)	1×10^{-5}	1×10^{-7}	4×10^{-4}	1.2×10^{-3}	5×10^{-1}	1×10^{-9}

*Air-entry values were computed using Zhai and Rahardjo (2012) equations.

∗ ϕ^b angle indicating the rate of change in shear strength relative to changes in matric suction, (u_a-u_w).

4 RESULTS AND DISCUSSION

Figure 6 shows the PWP variations predicted by the numerical analyses as compared to the field data. Both results indicate that, even under this heavy rainfall amount, there was very small variations in PWP in the compacted soil as well as in the fine and coarse layers. In general, the results of numerical analysis agree with the field data except for the PWP recorded by TM1, whereby numerical analyses indicated an increase in PWP after 3 days of intermittent rainfalls while the field data did not show significant increase. The field data suggested that the PWP in the compacted soil was between -18 and -22 kPa while the numerical analyses showed an increase in PWP in TM1 up to -7.2 kPa. This shows that only a small amount of rain-water infiltrated through the GBS slope even under a heavy rainfall condition. The PWPs recorded in the fine-grained material were slightly affected by the rainfall (fluctuated between -14.5 and -16.5 kPa) but the PWPs in the coarse-grained layer were almost constant at -4.5 kPa. This indicated that there was no breakthrough under the heavy rainfall from January 18th to 23rd 2017. The numerical analyses indicated an increase in PWP in the fine RAP up to -10 kPa and a slight increase in PWP in the coarse-grained layer to a maximum value of -2.2 kPa.

Figure 7 shows the total vertical and horizontal pressures predicted from the numerical analyses as compared to the monitoring data from the earth pressure cells in GBS slope 2. The numerical analyses predicted a more significant effect of rainfall infiltration as compared to the field data. However, the

magnitudes of vertical and horizontal stresses computed from the numerical analyses were comparable with the field data.

Slope stability analyses were carried out for two possible slip surfaces i.e. global failure of the wall whereby the whole system will slide along the slip surface below the GBS, and local failure in which the slip surface will form inside the GBS itself. Figure 8 shows the variation of Factor of Safety (FOS) with respect to the global and local slip surfaces shown in Figure 9a and 9b, respectively. Figure 8 indicated that the local stability of the GBS was not affected by rainfall infiltration because the system was protected by capillary barrier. The global stability was slightly affected by the rainfall because the residual soil behind the GBS was affected by rainfall infiltration and possible rise of GWL. However, the rainwater infiltration behind GBS did not affect the stability of the slope since the factor of safety of at the end of rainfall was still high (i.e., 2.35). The initial GWL in this site was quite shallow i.e. at a depth of 2.8m below the toe of the slope and it was raised to 0.7m below the toe due to the heavy rainfall on January 18th to 23rd 2017.

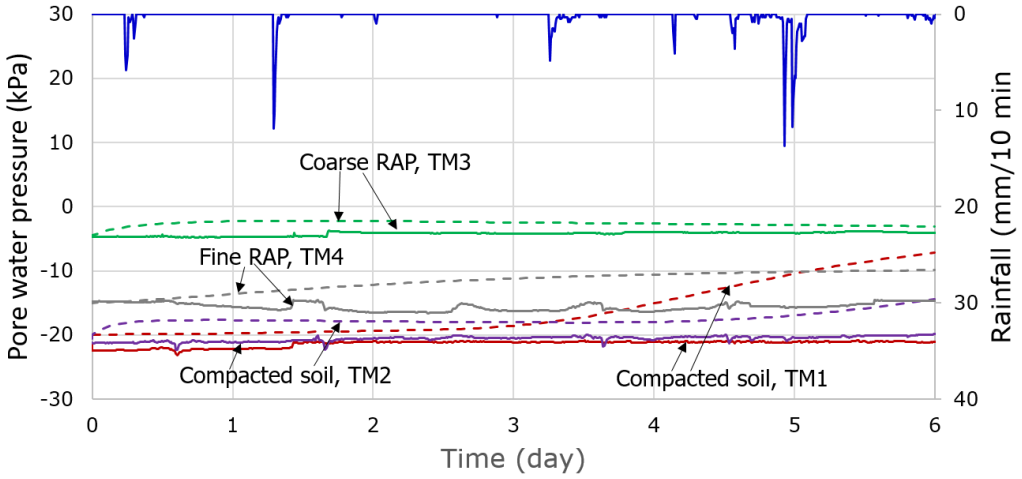

Note: dashed lines = numerical analysis data; solid lines = field data
day 0 = 00:00 on 18th January

Figure 6 PWP variations predicted by numerical analysis as compared to field data

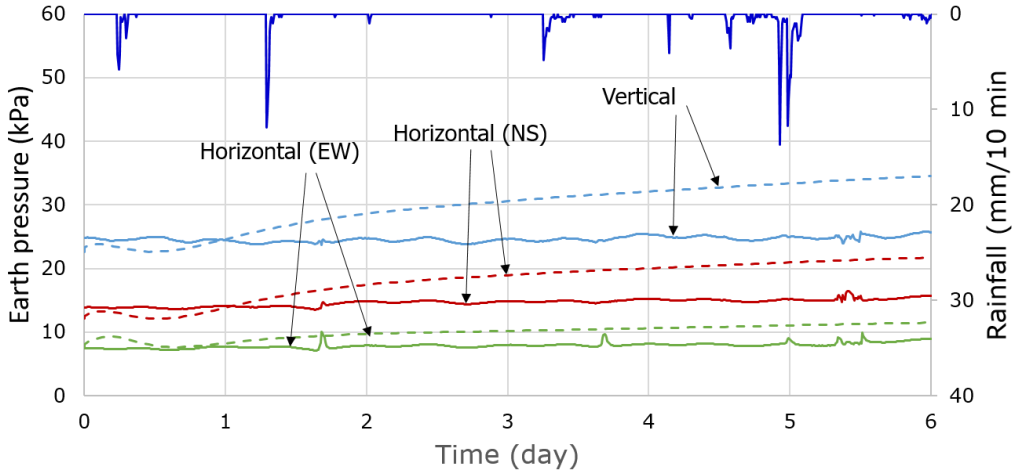

Note: dashed lines = numerical analysis data; solid lines = field data
day 0 = 00:00 on 18th January ; NS = direction from crest to toe ; EW = perpendicular to NS

Figure 7 Effect of rainfall infiltration on vertical and horizontal pressure in GBS slope 2

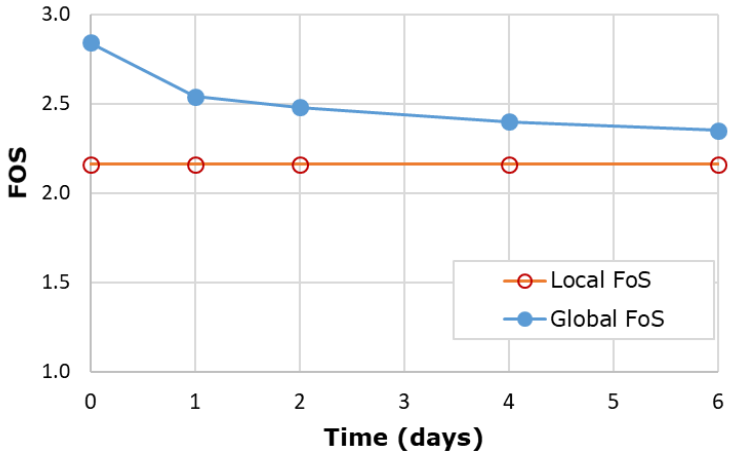

Figure 8 Variation of Factor of safety of GBS slope calculated by limit equilibrium method in SLOPE/W

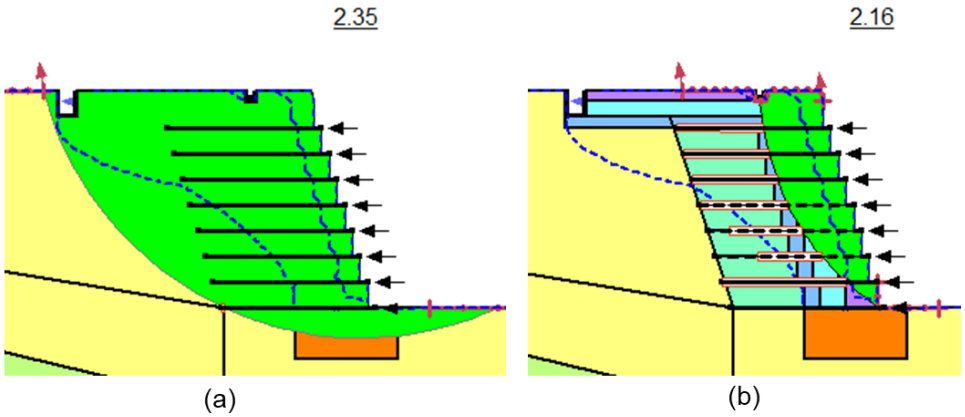

Figure 9 Failure planes developed in GBS slope 2 from (a) Global and (b) local stability analyses.

5 CONCLUSIONS

Numerical analyses have been carried out and the results were evaluated using field data to investigate the performance of GBS as a protection of a steep residual soil slope. The conclusions from this study are as follows:

1. The pore-water pressure variations predicted from the numerical analyses agreed with those obtained from the field data. This indicates that the numerical procedure using deformation and seepage analyses could be used to predict the pore-water pressure characteristics within the GBS slope, especially during rainfall infiltration.
2. The results from the numerical analyses and the field data showed that the effect of rainfall infiltration on the reinforced soil in the GBS slope was minimal. Hence, the GBS slope performed well in minimizing rainwater infiltration and maintaining the stability of the slope during rainfall.

REFERENCES

Geo-Slope International Ltd. 2012. SIGMA/W Stress deformation modelling. Geo-slope International Ltd., Calgary, Alberta, Canada.

Geo-Slope International Ltd. 2012. SLOPE/W for Slope Stability Analysis. Geo-slope International Ltd., Calgary, Alberta, Canada (2012b).

Harnas, F.R., Rahardjo, H., Leong, E.C., & Wang, J.Y. 2014. Experimental study on dual capillary barrier using recycled asphalt pavement materials. Canadian Geotechnical Journal. 51: 1165-1177.

Koerner, R.M. Koerner, G.R. 2013. A data base, statistics and recommendations regarding 171 failed geosynthetic reinforced mechanically stabilized earth (MSE) walls. Geotextiles and Geomembranes 40 (2013) 20-27

Koerner, R.M. 20012. Designing with Geosynthetics, 6th ed. Prentice Hall. 796 p.

Liu, C.N., Yang, K.Y., Ho, Y.H., Chang, C.M. 2012. Lessons learned from three failures on a high steep geogrid-reinforced slope. Geotextiles and Geomembranes 34: 131 – 143.

McCulloch, T., Kang, D., Shamet, R., Lee, S.J. and Nam, B.H. 2017. Long-Term Performance of Recycled Concrete Aggregate for Subsurface Drainage. Journal of Performance of Constructed Facilities, 31(4).

Rahardjo, H., Gofar, N., Harnas, F. Satyanaga, A. 2018. Effect of Geobags on Water Flow through Capillary Barrier System. Geotechnical Engineering Journal of the SEAGS & AGSSEA 49(2) June 2018

Rahardjo, H., Zhai, Q., Satyanaga, A., Leong, E.C., Wang, C.L. and Wong, L.H. 2015. Geo-Barrier System as a retaining structure. Proceedings of AP-UNSAT2015 Conference, 23-26 Oct 2015, Guilin, China, pp. 871-876.

Rahardjo, H., Satyanaga, A. Leong, E.C., and Wang, J.Y. 2013. Unsaturated Properties of Recycled Materials. Engineering Geology. 161: 44-54

Rahardjo, H., Santoso, V.A., Leong, E.C., Ng, Y. S. and Hua, C.J. 2012. Performance of an Instrumented Slope Covered by a Capillary Barrier System. ASCE Journal of Geotechnical and Geoenvironmental Engineering. 138(4):481-490.

Yoo, C. and Jung, H.Y. 2006. Case History of Geosynthetics Reinforced Segmental Retaining Wall Failure. Journal of Geotechnical and Geoenvironmental Engineering, 132(12): 1538-1548.

Zhai Q, Rahardjo H. (2012) Determination of soil–water characteristic curve variables. Computer and Geotechnics, 42:37–43.